



Analyzing in situ stresses and wellbore stability in one of the south Iranian hydrocarbon gas reservoirs

Alireza Sobhani¹ · Ali Kadkhodaie² · Majid Nabi-Bidhendi³ · Mehdi Tadayoni⁴

Received: 1 September 2022 / Accepted: 4 January 2024 / Published online: 3 February 2024
© The Author(s) 2024

Abstract

This study aims to analyze in situ stresses and wellbore stability in one of the Iranian gas reservoirs by using well log data, including density, sonic (compressional and shear slowness), porosity, formation micro-image (FMI) logs, modular formation dynamics tester (MDT), and rock mechanical tests. The high burial depth, high pore pressure, and strike-slip stress regime of the field require an optimal design of geomechanical parameters based on an integrated data set consisting of static and dynamic data, which is available for this study. Firstly, poroelastic modulus and vertical stress were calculated. Afterward, the Eaton's equation was used to estimate pore pressure from well logging data. The geomechanical parameters were also calibrated through the interpretation of image data, the use of the modular formation dynamics tester (MDT), and laboratory rock mechanic tests. Employing poroelastic equations, the lowest and highest horizontal stresses were calculated. It was shown that the maximum horizontal stress and minimum horizontal stress correspond to σ_H and σ_h , indicating the strike-slip fault regime. The findings of this research indicated that the equivalent mud weight (EMW) resulted in 10–13 ppg suitable for the Kangan Formation and 11–14 ppg suitable for the Dalan Formation. Additionally, the well azimuth in the NE-SW direction provided the best stability for drilling the encountered formations. Therefore, the results of this study serve as cost-effective tools in planning adjacent wells in carbonate formations of gas field to predict the wellbore stability and safe mud window.

Keywords Geomechanics parameters · Wellbore stability · Poroelastic modulus · In situ stresses

List of symbols

E	Young's modulus, GPa
E_{dyn}	Dynamic young's modulus, GPa
E_{sta}	Static young's modulus, GPa

g	Gravity, ft/ s ²
P_{pg}	Pore pressure gradient, psi/ft
P_p	Pore pressure, psi
S_g	Overburden pressure gradient, psi/ft
S_v	Overburden pressure, psi
U	Shear modulus, GPa
V_p/V_s	Compression-to-shear velocity ratio, dimensionless
Z and d_z	Depth, ft
α	Biot coefficient, dimensionless
Δt	Measured sonic transient time, $\mu\text{s}/\text{ft}$
ϵ_x	Linear strain elongation components on the direction x
ϵ_y	Linear strain elongation components on the direction y
ν	Poisson's ratio, dimensionless
ρ	Bulk density, kg/m^3
σ_H	Maximum horizontal stress, psi
σ_h	Minimum horizontal stress, psi
σ_v	Vertical stress, psi

✉ Alireza Sobhani
alirezasobhani1989@gmail.com

Ali Kadkhodaie
kadkhodaie_ali@tabrizu.ac.ir

Majid Nabi-Bidhendi
mnbhendi@ut.ac.ir

Mehdi Tadayoni
mtdadayoni@gmail.com

¹ Department of Petroleum Engineering, Tehran Science and Research Branch, Islamic Azad University, Tehran, Iran

² Earth Sciences Department, Faculty of Natural Sciences, University of Tabriz, Tabriz, Iran

³ Institute of Geophysics, University of Tehran, Tehran, Iran

⁴ Faculty of Petroleum and Renewable Energy Engineering, Universiti Teknologi Malaysia (UTM), Johor Bahru, Malaysia

Abbreviations

DITF	Drilling-induced tension fractures
DSI	Dipole shear sonic imager
DTCO	Delta-t compressional log
DTSM	Delta-t shear log
EMW	Equivalent mud weight
FMI	Formation micro-imager
LOT	Leak-off test
MDT	Modular formation dynamics tester
NPHI	Neutron porosity log
PIGN	Porosity log
POIS	Poisson's ratio
RFT	Repeat formation tester
RHOB	Density log
TSTR	Tensile strength
UCS	Unconfined compressive strength
WOB	Weight on bit
XLOT	Extended leak-off test

Introduction

In order to reduce the risks and costs related to the drilling operations, it is crucial to assess the stability of wellbores as part of a comprehensive field study (Ashena et al. 2020). In order to prevent mechanical failures in the wellbore, the process includes preventing chemical reactions between the drilling fluid and well fluid, ensuring a good drilling trajectory, and controlling the drilling parameter (Mondal and Chatterjee 2019). In most cases, drilling problems caused by unanticipated or unforeseen subsurface conditions cost time, money, and well destruction. The problem costs the oil business a lot of money every year (Awal et al. 2001; Bradley 1978). Many steps were taken to optimize such pricey issues as drilling fluid programs and casing programs (Kadkhodaie 2021). The advent of underbalanced drilling technology has led to concerns about how wells that enter horizontally and drill multiple laterals from one well can address these concerns (Awal et al. 2001; Kristiansen 2004; Martins et al. 1999; Tan et al. 2004). As long as drilling does not take place, the stress applied to the ground is less than the rock's strength, maintaining its equilibrium (Bagheri et al. 2021). A part of the rock column was deflected by the drilling and moved out of the well, which was then replaced by drilling mud and pushed against the wall of the wellbore (Bagheri et al. 2021). As a result, the ground stress equilibrium was disrupted and stress was generated by drilling (Bagheri et al. 2021). It is essential to maintain wellbore stability and regulate these stresses by using the optimal mud weight (Darvishpour et al. 2019). Instability in the wellbore occurs for a number of reasons, including mechanical failures (such as high-stress concentrations, low rock strength, or improper drilling methods) and chemical

interactions between the drilling fluid and the rock (most commonly clays) (Kadkhodaie 2021). Washout and wellbore wall failure are usually caused by a combination of mechanical and chemical factors (Kadkhodaie 2021). It is necessary to know the rock strength, select a suitable model, and define an appropriate rock failures criterion in order to determine wellbore stresses. Rock strength properties can be calculated from well logs and empirical equations (Peng et al. 2001; Rahimi 2014). A number of relationships are presented by Heller and Zoback that can be applied to unconfined compressible rocks (sandstones, carbonate rocks, and shale) (Heller and Zoback 2014). They depend on many variables, including sonic wave transit times, ultrasonic wave velocities, elastic moduli, and porosity (Hoseinpour and Riahi 2022). In recent years, several studies have investigated wellbore stability, geomechanical modeling, and associated parameters. Radwan discovered several different data sets and numerical methods to investigate pore pressure and fracture gradients (Radwan et al. 2019, 2020; Radwan 2021). They looked into the connection between in situ stress and reservoir characteristics related to wellbore stability, well decline, and flow rate in addition to reservoir geomechanical modeling (Radwan et al. 2021; Radwan and Sen 2021a, b). According to research by Radwan, there are many different ways to estimate in situ stresses (Radwan 2021; Radwan and Sen 2021a, b). Gholami's study in the Canning Basin, Australia, focused on geomechanical parameters and stress levels for wellbore stability analysis (Gholami et al. 2017). In a study conducted by Han, the researchers described three steps for determining the poroelastic properties of fractured rocks: measurement, analysis, and interpretation (Han et al. 2019). Khatibi calculated the single-parameter parabolic failure criterion by applying triaxial strength, a geomechanical model of the Iranian oil field, and uniaxial compressive strength estimates (Khatibi et al. 2018). Haimson and Kovacich studied fracture-like breakouts as a mechanism to resolve the wellbore instability associated with porous Berea sandstones (Haimson and Kovacich 2003). Kassem determined the geomechanical parameters of a sandstone reservoir to determine the effect of fluid injection and depletion (Kassem et al. 2021). A shallow unsupported wellbore based on the Drucker–Prager failure criteria was analyzed by Hashemi to create geomechanical models (Hashemi et al. 2014). Carbonate reservoirs have a complex pore system and fractures as compared to clastic reservoirs. Therefore, it is very important to be able to predict pore pressure effectively due to the complexity of the pore system and fractures. Additionally, pore pressure has a direct impact on drilling parameters such as weight on bit, which has a direct effect on drilling rate. Moreover, geomechanical studies also take into account the pore pressure and rock strength parameters (Khoshnevis-zadeh et al. 2021). Khoshnevis-zadeh concentrated on the K4 member of the Dalan Formation by using

drilling data such as weight on bit (WOB) to measure and compare the dynamic parameters calculated by well log instead of core data. Thus, the porosity and density of the rock in the wellbore are directly correlated; both of those variables are impacted by the strength of the wellbore and the depth of penetration (Khoshnevis-zadeh et al. 2019).

Studies on well stability and geomechanical parameters in carbonate formations have not been sufficiently extensive. This study specifically focuses on estimating mud weight by using geomechanical parameters to determine the accuracy of elastic moduli using laboratory tests and well log data from the Kangan and Dalan Formations. Additionally, safe drilling deviation trajectory standards are being developed using these findings. The outcome of this study can potentially be used to arrive at a good development plan, and the overall well development can be optimized through the use of the best engineering design in the carbonate formation.

Study area

The South Pars gas field is located in the Persian Gulf in Iran's southern part. In the South Pars gas field, the well that was studied is located. Our study was conducted on the Kangan and Dalan Formations. The Dalan and Kangan Formations are of late Permian and early Triassic age, respectively, and both are composed primarily of carbonate rocks. The Dalan and Kangan are, respectively, late Permian and early Triassic, and carbonated lithology dominates both formations (Rahimpour-bonab 2007). Accordingly, the reservoir zone can be divided into four distinct sections, depending

on the stratigraphic aspects, and these sections are known as K1, K2, K3, and K4 (Khoshnevis-zadeh et al. 2021). Accordingly, sections K1 and K2 belong to the Kangan Formation, and sections K3 and K4 belong to the Dalan Formation (Khoshnevis-zadeh et al. 2021). Specifically, the majority of hydrocarbons are found in the upper Dalan and Kangan Formations, which are equivalent to the upper Khuff Formation (Esrafilidizaji and Rahimpour-bonab 2019). Figure 1 illustrates the location of the study area and the stratigraphic column of that area.

Materials and methods

The conventional well logs, which include density, sonic logs porosity together with formation micro-image (FMI), are used in this study. Additionally, data were obtained from rock mechanical tests including uniaxial compressive strength tests, unconfined modulus of elasticity, Poisson's ratio, and pore pressure values gathered from modular dynamic tester instruments. This study presents geomechanical analyses derived from well log data and direct downhole measurements in one well. The standard well logs used in the geomechanical model are depicted in Fig. 2. From left to right, they are as described as follows: The first track shows the delta-t compressional log. Delta-t shear log is represented on the second track, neutron porosity log on the third, and formation density log on the fourth track.

The best drilling and completion methods can be estimated and predicted using a geomechanical model, either for drilling within a borehole or for developing a field (Ashena

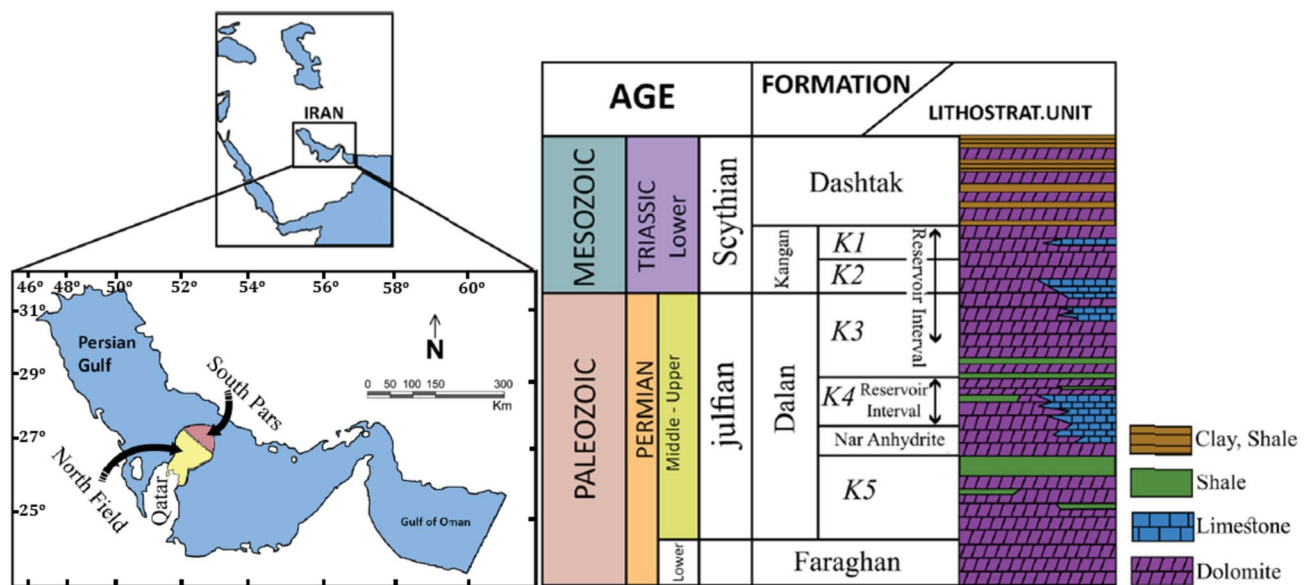


Fig. 1 The map to the left shows the location of the studied area, while that to the right shows the general stratigraphy of the South Pars gas field (Rahimpour-bonab 2007)

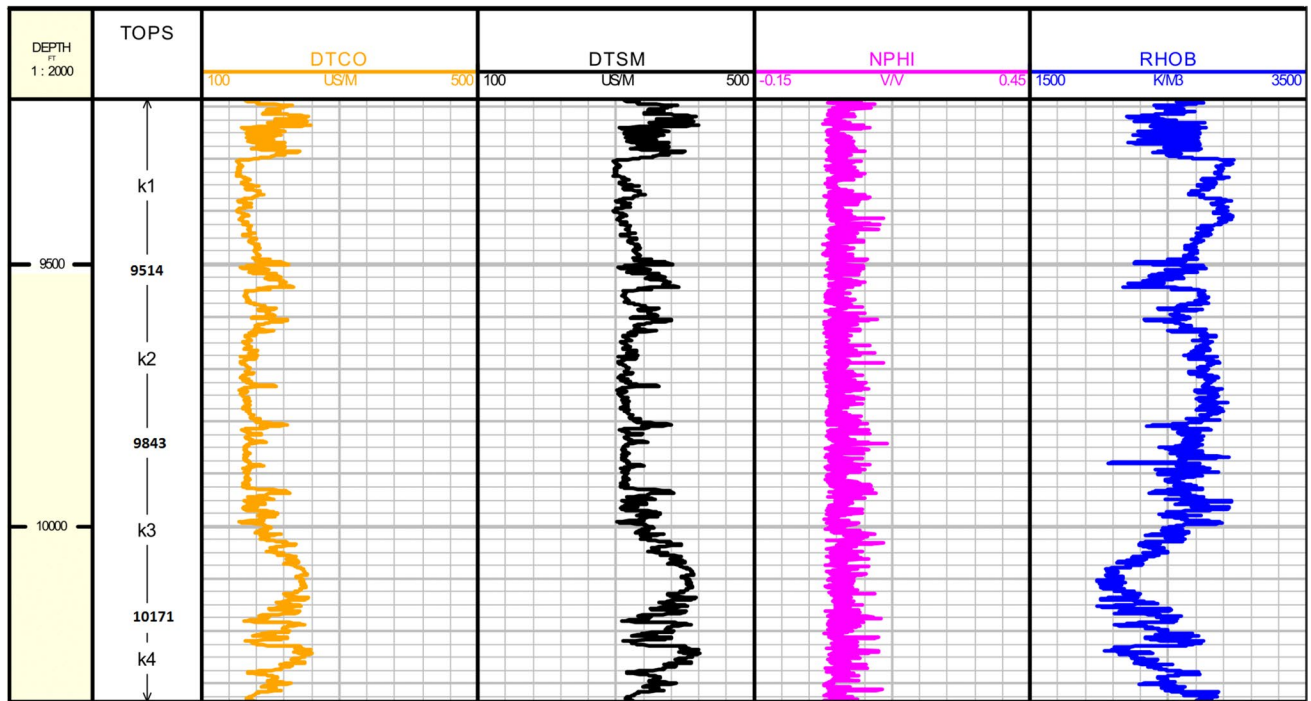


Fig. 2 Petrophysical logs were used for the geomechanical model in the Kangan and Dalan Formations

et al. 2022). Figure 3 shows the workflow and general steps used in this work.

Rock elastic parameters

An analysis of density and acoustic logs can determine a variety of rock strength parameters, including Young's modulus, Poisson's ratio, bulk modulus, and shear modulus (Khoshnevis-zadeh et al. 2019). Empirical equations were used to convert the calculated parameters into static modules (Khoshnevis-zadeh et al. 2019).

Rock strength

Rock resistance to in situ stresses around the wellbore is referred to as rock strength. Unconfined compressive strength (UCS) is a frequently used indicator of the power of rocks. For UCS calculations, measurements from records are typically utilized. Unconstrained compression tests or multistage triaxial compression tests on cores are frequently used to calibrate continuous logs at a single location. Equation 1 can be used to determine the UCS. Tensile strength (TSTR) is calculated by dividing UCS by a predetermined factor. It typically ranges from one-eighth to one-twelfth of UCS (Zoback 2010). Here, tensile strength is equivalent to one-tenth of uniaxial compression strength.

$$UCS = \frac{7682^{1.82}}{145} \Delta t \quad (1)$$

where Δt is the measured sonic transit time in $\mu\text{s}/\text{ft}$.

Static Young's modulus and unconfined compressive strength

Laboratory test results were used to calibrate static data generated from dynamic data (static values). We determined the static Young's modulus and unconfined compressive strength in the examined field using Eqs. 2 and 3, as well as earlier research and laboratory experiments.

$$E_{\text{sta}} = (-2.21 \times \text{PIGN} + 0.963) \times E_{\text{dyn}} \quad (2)$$

$$UCS_{\text{sta}} = (3 + 4.1 \times E_{\text{sta}}) \times 145 \quad (3)$$

where E_{sta} = static Young's modulus; E_{dyn} = dynamic Young's modulus; PIGN = porosity log.

Accordingly, in this study, ASTM D 3148–93 and ISRM suggested methods were considered. Briefly, a rock core specimen was cut to length and the ends were machined flat. The specimen was placed in a loading frame. In addition, axial and lateral deformation were monitored as a function of load on the specimen, as axial load continuously increased. The specimens were tested at room temperature

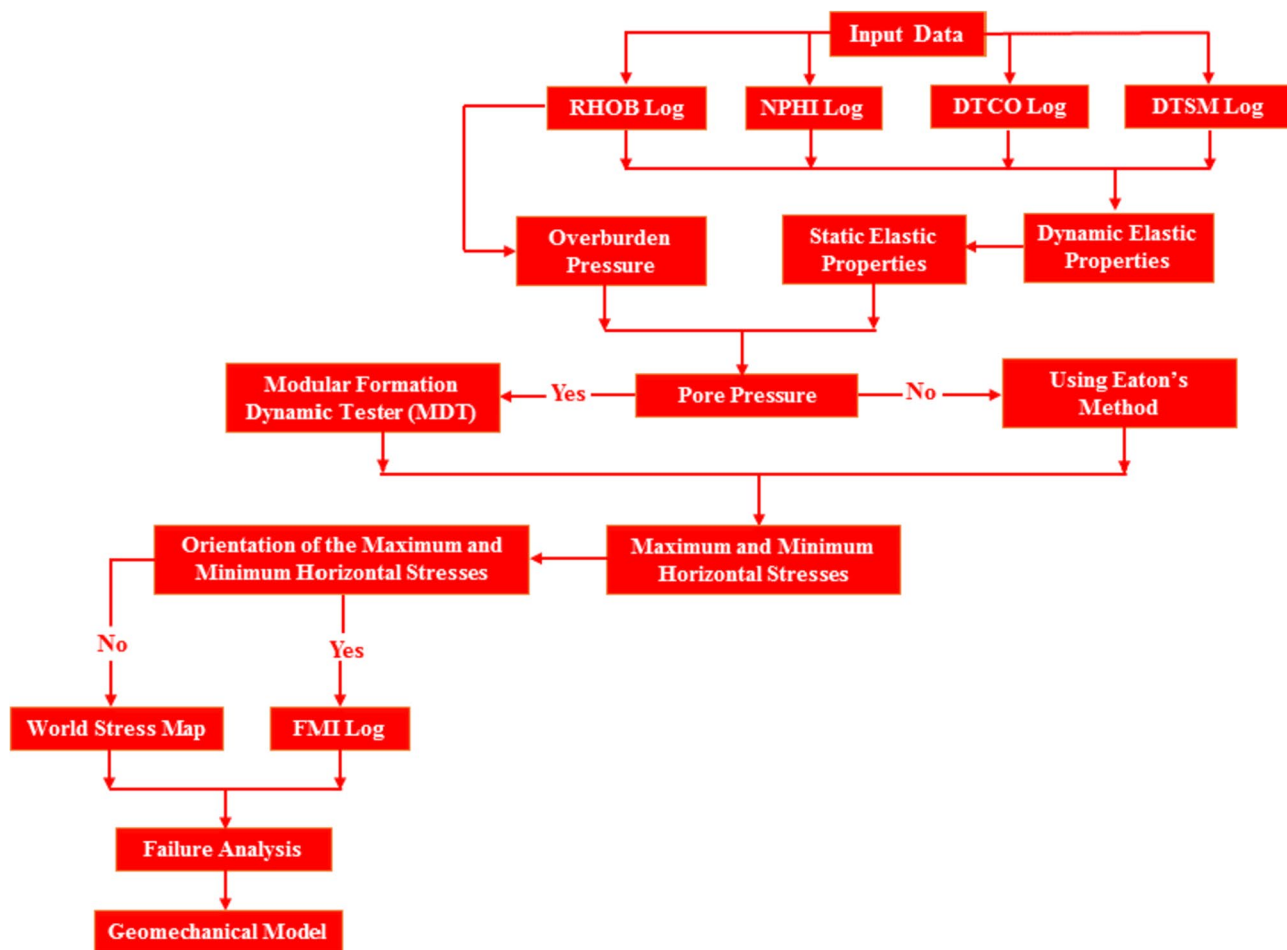


Fig. 3 Step-by-step process for building a geomechanical model

under dry conditions. In order to preserve natural conditions, specimens from the reservoir were not washed. The specimens were tested at a stress rate of 0.75 to 1.0 MPa/s.

In Table 1, the results of the uniaxial compressive strength test, elasticity modulus, and Poisson’s ratio measurement are listed.

Overburden pressure

Pressure profiles are created by combining the vertical column pressures of various rocks with the pore pressures in overburden stress (Almalikee and Al-najim 2018). In subsurface studies, the overburden pressure is affected by different factors,

such as the weight of upper layers and porosity of the rock, density of fluids in the pores, diagenetic impact, and tectonic factors. Overburden pressure is determined by the thickness of the bed and density of the bed (Zoback 2010). According to Eq. 4, it was calculated (Zang and Stephansson 2009).

$$S_v = \int_0^z \rho_z g dz \cong \bar{\rho} g z \tag{4}$$

Rock density is ρ and z is formation thickness, respectively.

Table 1 The results of the uniaxial compression test plus unconfined modulus of elasticity and Poisson’s ratio determination

Sample Set	Sample No	Depth (m)	σ_c (MPa)	E (GPa)	ν	Length (mm)	Diameter (mm)
3	RM3C	3069.42	4.46	12.27	0.37	78.41	37.63
	RM3D	3069.50	4.89	9.81	0.21	78.77	37.72
	RM3	3069.08	2.90	5.97	0.15	137.99	52.89
	Average		4.08	9.35	0.25		

For intervals without density logs, the vertical stress was calculated by averaging the densities of subsurface formations in relation to lithology (Kadkhodaie 2021).

Prediction of the pore pressure

Typically, pore pressure is measured using a repeat formation tester (RFT), a modular dynamics test (MDT), well test analysis, and logging while drilling sensors (Ashena et al. 2020). There are a large number of carbonate reservoirs worldwide, particularly in the Middle East (Khoshneviszadeh et al. 2021). Thus, the compaction trend in carbonate rocks is influenced both physically and chemically by a variety of parameters, including pore system complexity, diversity extent, and the determination of pore structure (Croizet et al. 2013). The pore pressure gradient was expressed by the Eaton sonic equation using Eq. 5 (Azadpour et al. 2015).

$$P_{pg} = S_g - (S_g - 0.86) \left(\frac{50 + (185 - 50)e^{-0.00137z}}{\Delta t} \right)^{0.45} \quad (5)$$

where S_g is the vertical stress gradient, Δt is the measured sonic transit time, and z is depth.

Discussion of results

In the current study, a complete set of subsurface data including conventional and advanced well logging data, core data, rock mechanical test results and formation test (MDT) data were integrated to make an optimal geomechanical model for the Permian–Triassic gas reservoirs of the world's largest non-associated gas field, Persian Gulf. For this purpose, firstly dynamic geomechanical properties were calculated using density (RHOB), compressional sonic, compressional wave velocity (V_p), and shear wave velocity (V_s) logs (Radwan et al. 2021) (Fig. 4). As is seen, the following tracks from left to right are shown, respectively: P wave modulus (track 1), shear modulus (track 2); Bulk's modulus (track 3); Poisson's ratio (track 4), the compression to shear velocity ratio (track 5) and Young's modulus (track 6). Afterwards, UCS and TSTR were estimated to plan the mud weight window, analyze wellbore stability and bit selection (Khoshneviszadeh et al. 2019) (Fig. 5). An optimal pore pressure prediction is essential to determining the magnitude of horizontal stresses (Radwan et al. 2021). As shown in Fig. 6, the pore pressure gradient calculated by Eaton sonic equation was compared with the modular formation dynamic tester (MDT) available for Kangan and Dalan Formations.

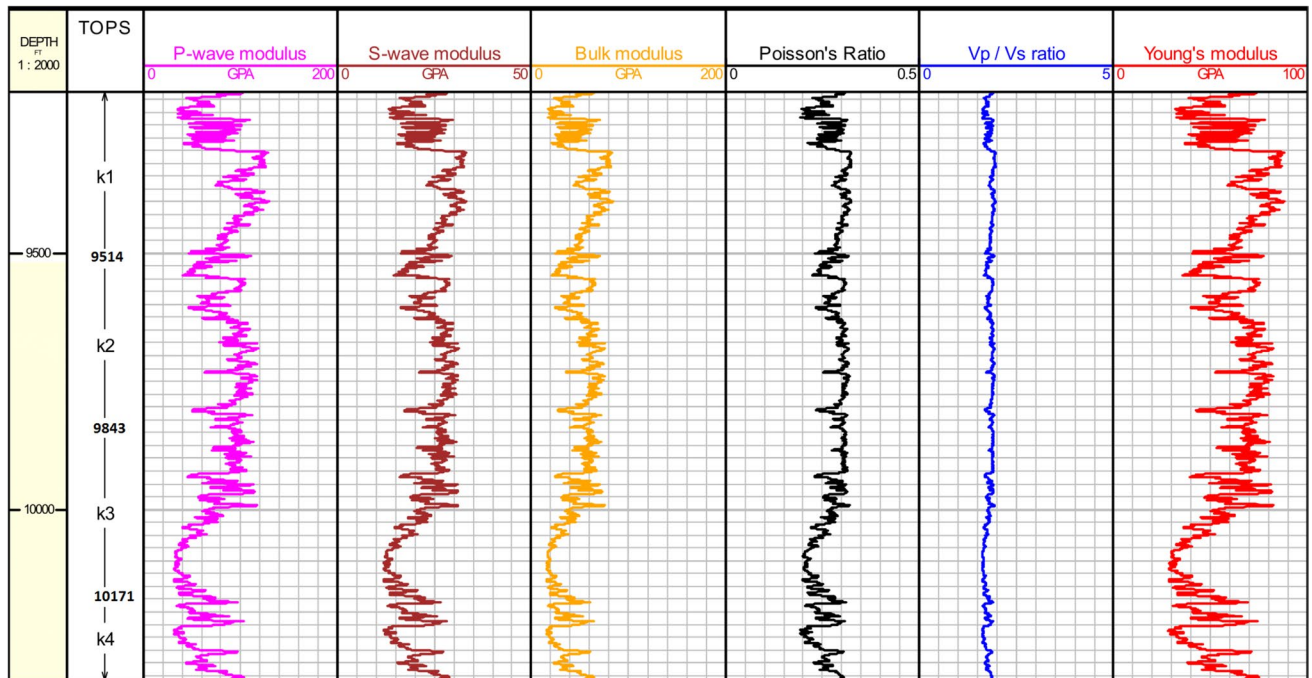
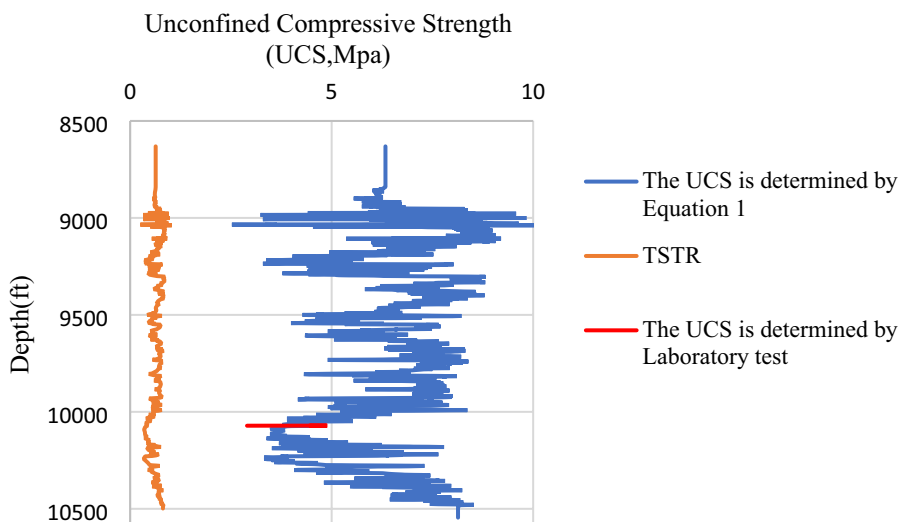


Fig. 4 A dynamic elastic parameters calculation was performed on the Kangan and Dalan Formations

Fig. 5 The UCS and TSTR were calculated by empirical equations and laboratory test



Pore Pressure Gradients

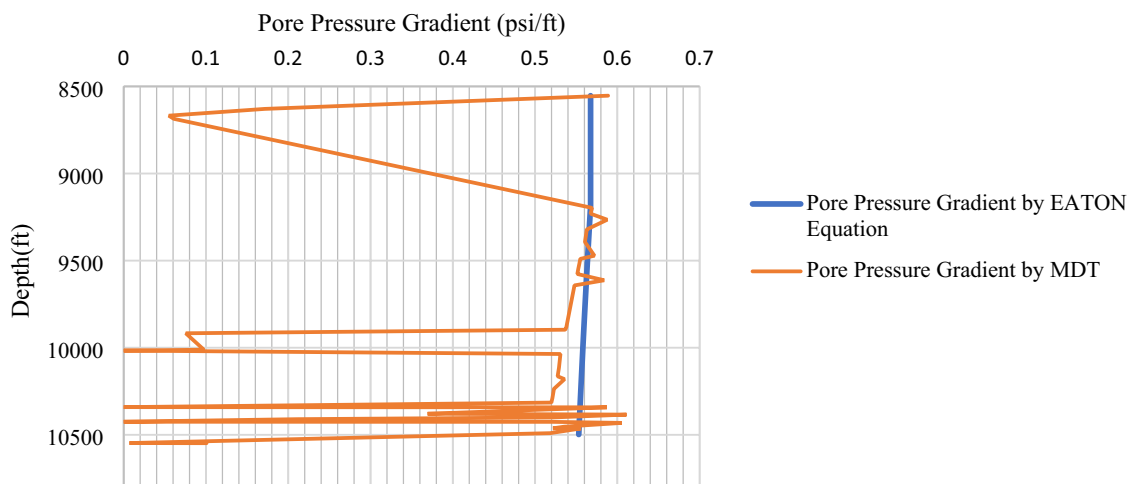


Fig. 6 The pore pressure gradients were calculated from Eaton’s method and calibrated with MDT results

Prediction of the minimum and maximum horizontal stresses

Prediction of minimum and maximum horizontal stresses is complicated and some approximations must be made. The poroelastic hypothesis was frequently used to determine the magnitude of horizontal stresses. According to the poroelastic theory, pressure-induced deformation of porous media results in volume changes. Applying this process to reservoir rocks with fluid-saturated pores within the elastic matrix is an especially effective strategy. Such a pore pressure changes caused by saturating pore fluids help to promote pore fluid flow in porous media as well as stiffen the material (Kadkhodaie 2021). Viscous fluids have a time-dependent reaction in porous media systems. Stresses and strains resulting

from tectonic plate movement are encountered in tectonically active basins. When tectonic strains are applied to rock formations, they add stress to elastic rocks (Abdideh and Fathabadi 2013).

In order to calculate the minimum horizontal stress, the following equations based on poroelastic theory (Eqs. 6, and 7) were used.

$$\sigma_h = \frac{\nu}{1 - \nu} (\sigma_v - \alpha P_p) + \alpha P_p + \frac{E \epsilon_y}{1 - \nu^2} + \frac{E \epsilon_x}{1 - \nu^2} \tag{6}$$

$$\sigma_H = \frac{\nu}{1 - \nu} (\sigma_v - \alpha P_p) + \alpha P_p + \frac{E \epsilon_x}{1 - \nu^2} + \frac{E \epsilon_y}{1 - \nu^2} \tag{7}$$

ε_x and ε_y are the linear strain elongation components on the “x” and “y” axis directions, respectively, α represents Biot’s coefficient (was set to 1). In Fig. 7, the horizontal stresses, as well as the vertical stress, are illustrated (Eaton 1976). The minimum horizontal stress (σ_h) was recalculated based on drilling evidences such as mud loss and appearance of shear and tensile fractures in the wellbore as well as the strain coefficients of ε_x and ε_y were adjusted until they reached optimal values meeting the stress regime model (Talebi et al. 2018). This equation predicts that the borehole breakout will initiate along the azimuth of σ_h when the maximum effective circumferential stress at the borehole exceeds the compressive rock strength (Moos and Zoback 1990).

Field stress regime analysis

According to the world stress map and regional tectonic studies, strike-slip faults are the predominant stress regime (Bozorgi et al. 2016). Anderson’s fault classification for strike-slip fault systems predicted that the magnitude of the maximum horizontal stress would be greater than the

magnitude of the vertical stress and minimum horizontal stress (Fig. 8), respectively ($\sigma_H > \sigma_v > \sigma_h$) (Kadkhodaie 2021). Identifying the maximum horizontal stress orientation and minimum horizontal stress orientation can be established from the FMI log. By contrast, breakouts are generally directed along the path of least horizontal stress (σ_h), while induced fractures are generally directed along the path of maximum horizontal stress (σ_H) (Kadkhodaie 2021). Figure 9 indicates that maximum stress is located in azimuths of 30° and 240° (NE–SW direction) based on FMI logs interpretation. There were breakouts (Fig. 10) in azimuths 60° and 330° (NW–SE) illustrating the direction of the minimum horizontal stress.

Three types of borehole instability factors exist, including chemical, mechanical and combinations of both. A mechanical factor is mainly determined by the weight of the mud (too light or too heavy) and the drilling method (depth, vibration, and lifting of pipes), whereas a chemical factor is greatly influenced by the drilling mud, namely inappropriate mud and insufficient inhibitors. The cause of borehole instability is usually a combination of chemical and mechanical factors. There is always pressure on underground structures due to vertical and tectonic stresses. During the drilling of a borehole in a geologic structure, some materials (rock) are taken out of the borehole. Only fluid pressure maintains the side walls of a borehole. As a result of inconsistencies between fluid pressure and the principal in situ stresses, new stress redistributions occur around the borehole, causing rock fractures. To analyze borehole stability issues, it is essential to identify the stresses present around the borehole. Borehole fractures can be divided into two types: drilling-induced tension fractures (DITF) and breakout fractures (Abdideh and Fathabadi 2013). Accordingly, the proper mud weight should be greater than the pore pressure to avoid formation collapse. In other words, formation’s horizontal stress and failure pressure should not be less than its mud weight as shown in Fig. 11. To estimate the elastic properties of the rock, data from logs, including sonic (DT), bulk density (RHOB), and a formation micro-image (FMI), were taken from 8631 to 10,545.5 ft of well A in the study area. Overall, various types of data were used, including formation test, well logs and rock mechanical tests. In this study, it was conducted using the STABView software for building a geomechanical model. Data sets were imported into this software are shown in Table 2.

Figure 12 represents the drilling mud weight (equivalent to collapse pressure) in black. When drilling fluid pressure drops below the black line, causes the wellbore to collapse, increasing or decreasing the diameter of the wellbore. A shear failure may occur at low levels of least mud weight, referred to as collapse pressure. Shear failure occurs at greater depths, while tensile failure occurs near the surface at the shallower depths. Loss of circulation increases the

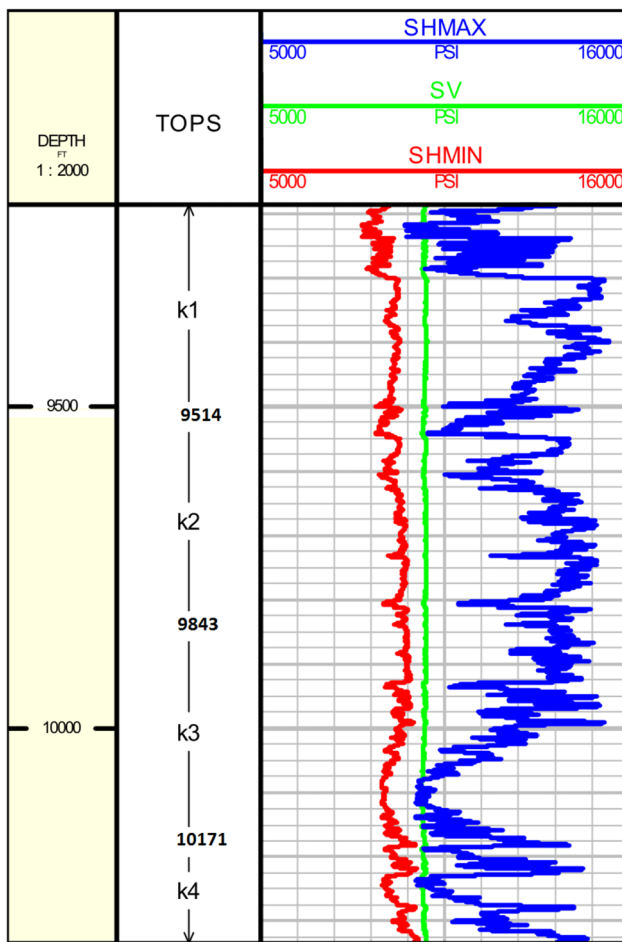


Fig. 7 The horizontal stresses and vertical stress profiles in well A

Fig. 8 An example of a borehole breakout and a drilling-induced fracture. There are equations related to the minimum and maximum hoop stresses (Fjær et al. 2008)

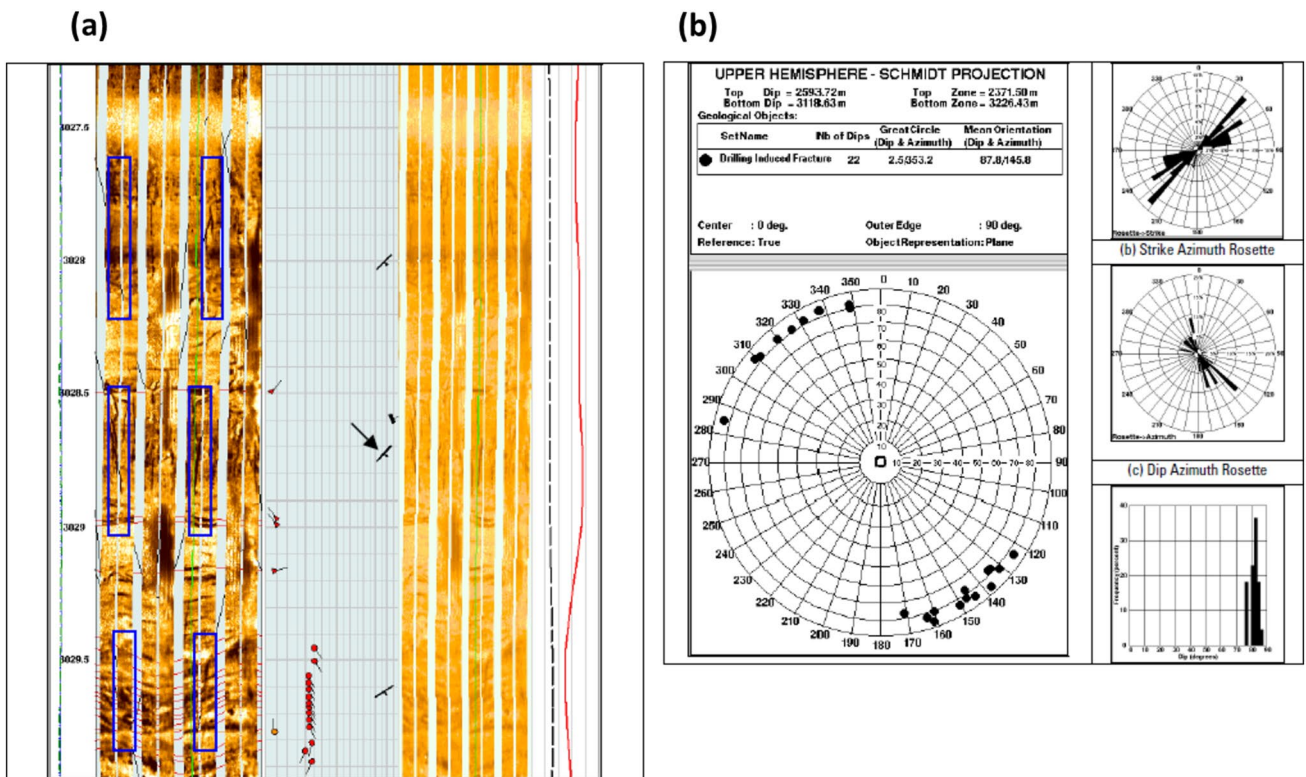
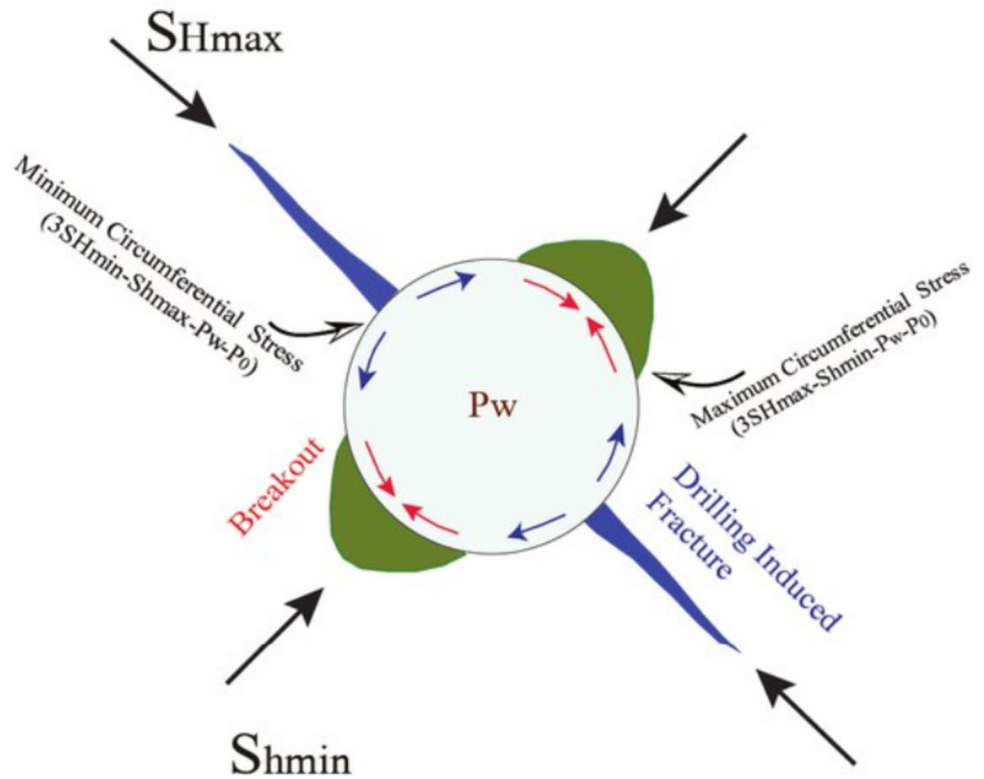


Fig. 9 Observed induced fractures on the FMI log (a) and rose diagram showing the induced fractures orientation (b) in well A

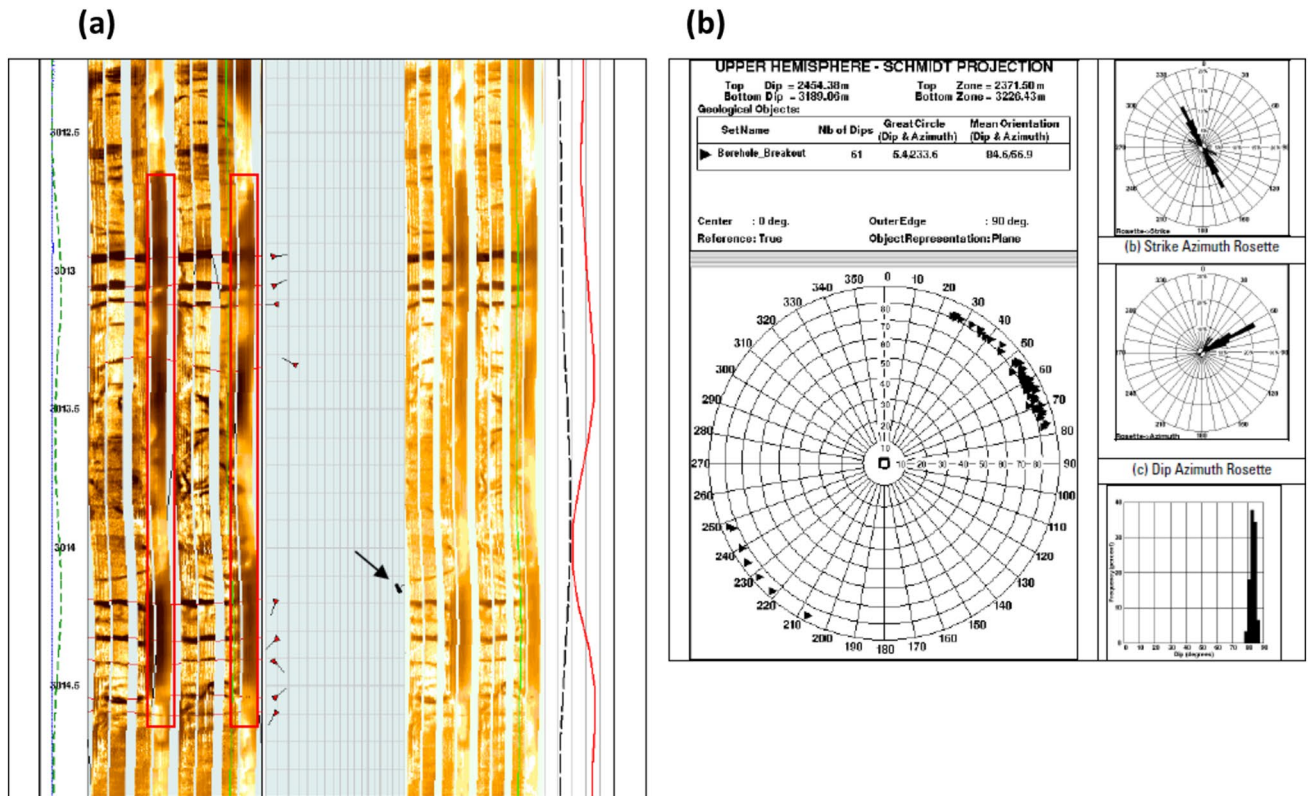


Fig. 10 Observed breakouts on the FMI log (a) and rose diagram showing the breakouts orientation (b) in well A

Fig. 11 The safe mud window is defined as the pressure between pore pressure and minimum horizontal stress (Abdideh and Dastyaft 2022)

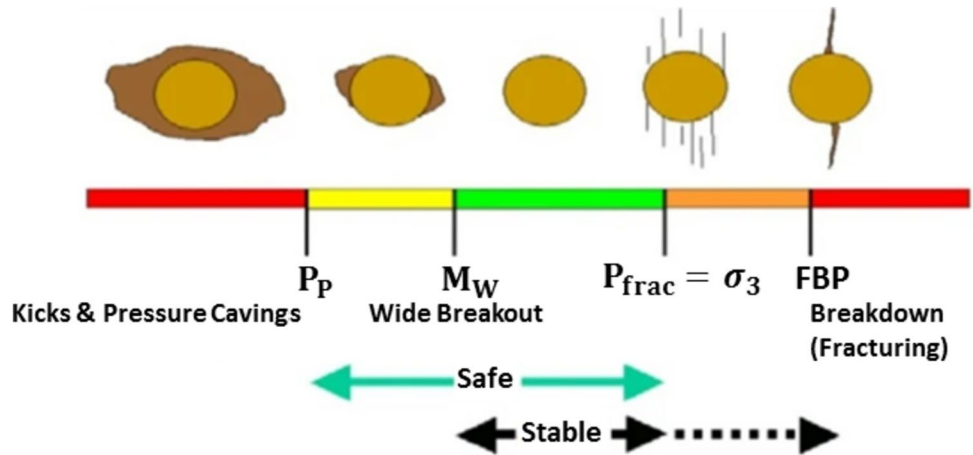


Table 2 The data sets were used to build geomechanical model

Pore Pressure (psi)	Minimum horizontal stress (psi)	Vertical stress (psi)	Maximum horizontal stress (psi)	Section
5279	9085	10,289	11,550	k ₁
5468	9075	10,288	11,500	k ₂
5613	9959	10,910	11,861	k ₃
5773	10,189	11,381	12,573	k ₄

probability of drilling fluid entering formations. Tensile failure ranges with a higher amount are known as fracture pressures (Gao et al. 2019a, b, c). Mohr–Coulomb failure criteria and two parameters are often used to determine shear strength. These are failure envelope cohesion and internal friction angle (Hoseinpour and Riahi 2022). According to Figs. 13, 14, 15, and 16, drilling direction and mud weight can provide an indication of the stability and instability of certain depths along the examined well. Using stereonets,

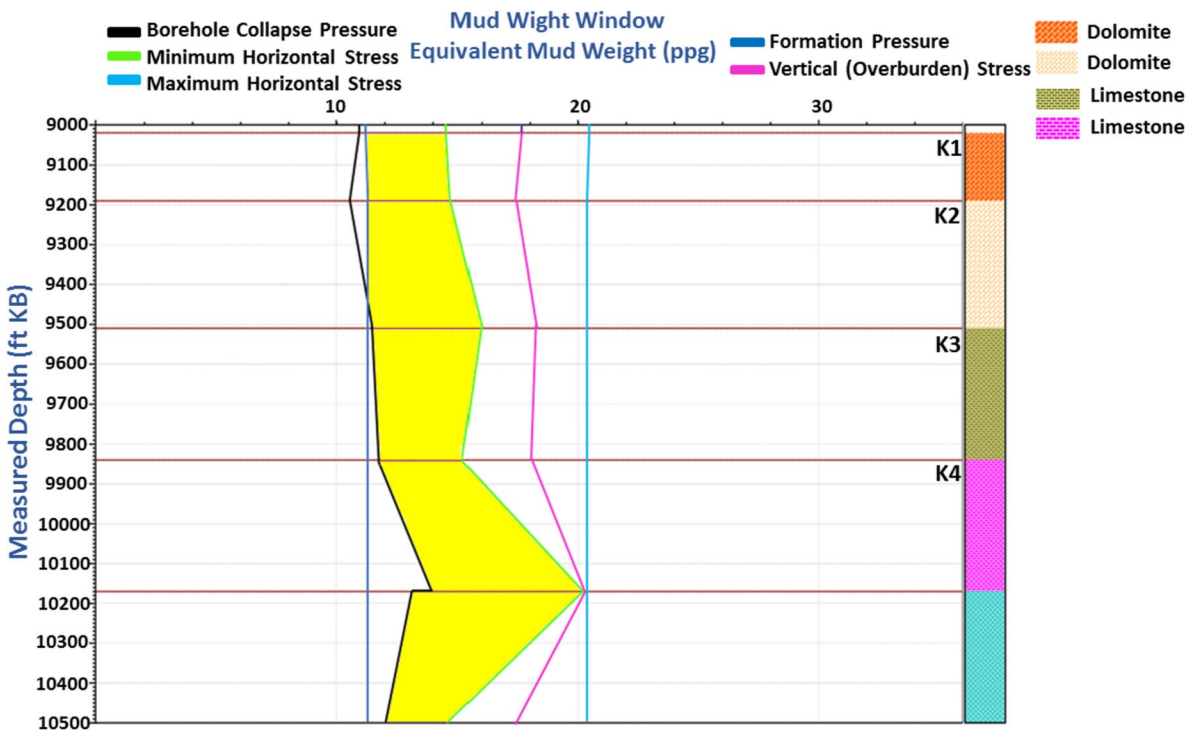


Fig. 12 The drilling safe weight window in the study area is shown in yellow for the Kangan and Dalan Formations. Mohr–Coulomb failure criteria used to determine the wellbore trajectory, which is determined by fracture gradient, drilling pressure, and mechanical conditions

Fig. 13 Polar plot showing required mud weight at different azimuths, K1 member of Kangan Formation

Analysis Mode: Pressure
Analysis Type: Drilling Collapse

Depth TVD = 9093.81 ftKB
Depth MD = 9093.81 ftKB
Formation: K1
Lithology: dolomite

Model: 3D Linear Elastic
Failure Criteria: Lade

σ_v grad = 1.13 psi/ft
 $\sigma_{H \max}$ grad = 1.27 psi/ft
 $\sigma_{H \min}$ grad = 1.00 psi/ft
 $\sigma_{H \min}$ Azi = 120°

P_r = 5362 psi

ϵ_{fc} = 0.00
 C_p = 2219 psi
 ϕ_p = 30°
 S_1 = 3843 psi
 $n(\eta)$ = 14.67
 E = 14.56 E+06 psi
 ν = 0.25
 α = 1.00

Effect of Well Trajectory on Collapse EMW

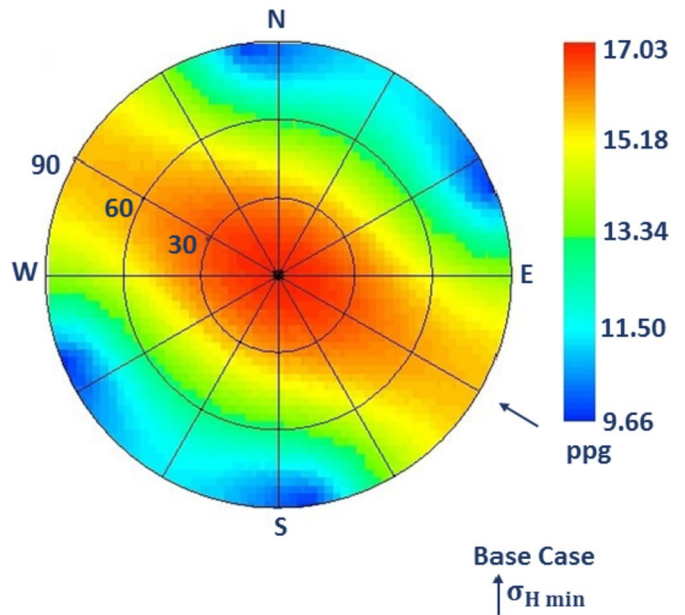


Fig. 14 The wellbore inclination and azimuth affect the mud weight window in K2 member, Kangan Formation

Analysis Mode: Pressure
Analysis Type: Drilling Collapse

Depth TVD = 9331.81 ftKB
Depth MD = 9331.81 ftKB
Formation: K2
Lithology: dolomite

Model: 3D Linear Elastic
Failure Criteria: Lade

σ_v grad = 1.13 psi/ft
 $\sigma_{H \max}$ grad = 1.25 psi/ft
 $\sigma_{H \min}$ grad = 1.01 psi/ft
 $\sigma_{H \min}$ Azi = 120°

P_r = 5532 psi

ϵ_{fc} = 0.00
 C_p = 2219 psi
 ϕ_p = 30°
 S_1 = 3843 psi
 $n(\eta)$ = 14.67
 E = 10.19 E+06 psi
 ν = 0.24
 α = 1.00

Effect of Well Trajectory on Collapse EMW

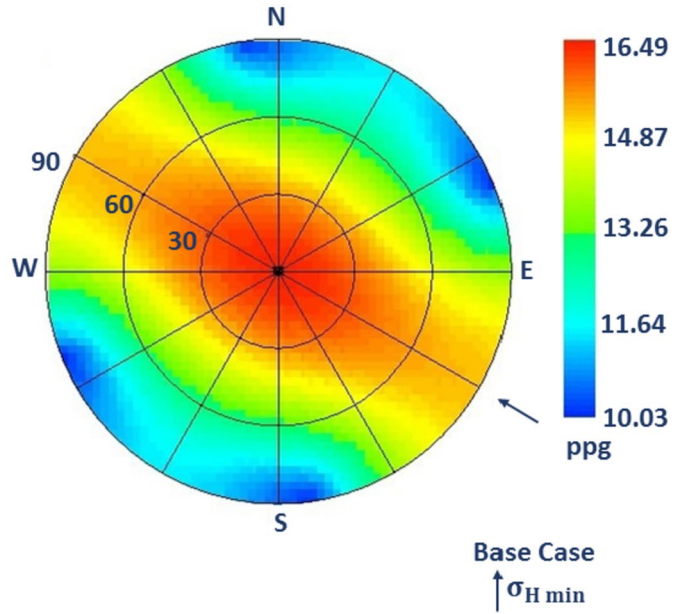


Fig. 15 The maximum and minimum horizontal stresses in K3 member, Dalan Formation

Analysis Mode: Pressure
Analysis Type: Drilling Collapse

Depth TVD = 9670.08 ftKB
Depth MD = 9670.08 ftKB
Formation: K3
Lithology: limestone

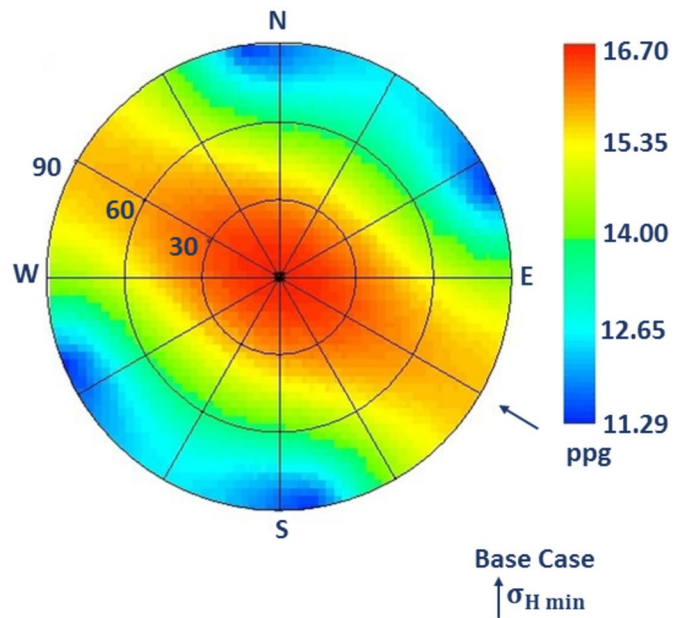
Model: 3D Linear Elastic
Failure Criteria: Lade

σ_v grad = 1.15 psi/ft
 $\sigma_{H \max}$ grad = 1.26 psi/ft
 $\sigma_{H \min}$ grad = 1.04 psi/ft
 $\sigma_{H \min}$ Azi = 120°

P_r = 5620 psi

ϵ_{fc} = 0.00
 C_p = 2219 psi
 ϕ_p = 30°
 S_1 = 3843 psi
 $n(\eta)$ = 14.67
 E = 8.41 E+06 psi
 ν = 0.32
 α = 1.00

Effect of Well Trajectory on Collapse EMW



the blue color represents locations where drilling orientations are safe (stable orientations), and the red color indicates unfavorable conditions (unstable orientations). A point

on the figures (Figs. 13 through 16) indicates the depth at which mud is employed. It is necessary to specify the optimal deviation, azimuth, and mud weight in order to prevent

Fig. 16 The inclination and azimuth of the wellbore affect the mud weight window in K4 member, Dalan Formation

Analysis Mode: Pressure
Analysis Type: Drilling Collapse

Depth TVD = 10008.35 ftKB
Depth MD = 10008.35 ftKB
Formation: K4
Lithology: limestone

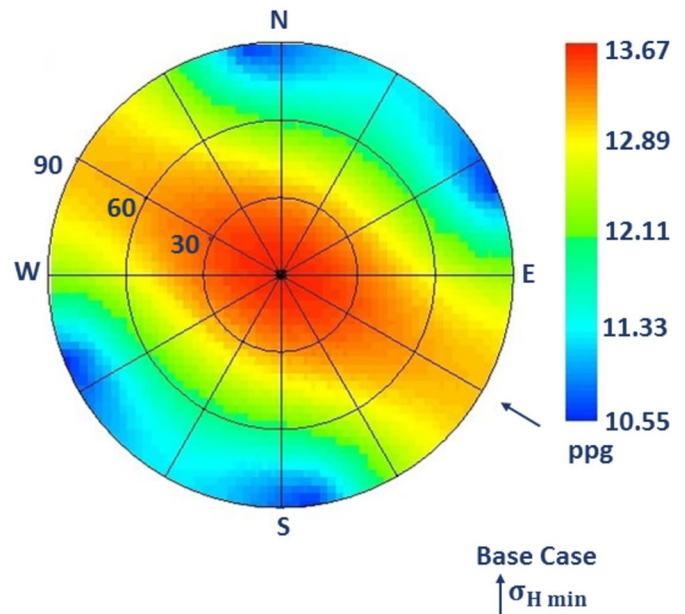
Model: 3D Linear Elastic
Failure Criteria: Lade

σ_v grad = 1.11 psi/ft
 $\sigma_{H \max}$ grad = 1.17 psi/ft
 $\sigma_{H \min}$ grad = 1.05 psi/ft
 $\sigma_{H \min}$ Azi = 120°

P_r = 5782 psi

ϵ_{fc} = 0.00
 C_p = 2219 psi
 ϕ_p = 30°
 S_l = 3843 psi
 $n(\eta)$ = 14.67
 E = 10.29 E+06 psi
 ν = 0.29
 α = 1.00

Effect of Well Trajectory on Collapse EMW



tensile and shear failures. Polar plots in the STABView are shown in Figs. 13, 14, 15, and 16.

In the Kangan Formation, deviations greater than 50° may cause various problems, including wellbore breakdown. Therefore, the safe mud weight window for drilling in the K1 and K2 members of the Kangan Formation is from 9.66 to 11.55 ppg and 10.03 to 11.64 ppg, respectively, at an azimuth of 277° and inclination of 35° (Figs. 13 and 14).

In the Dalan Formation, the minimum horizontal stress (σ_h) direction is NE-SW, while the maximum horizontal stress (σ_H) direction is NW-SE. In the Dalan Formation, drilling at more than 60° inclinations can cause wellbore breakout problems. As a result, the equivalent mud weight window for the K3 and K4 members of the Dalan Formation is 11.29 to 12.65 ppg and 10.55 to 11.33 ppg, respectively, with 45° of drilling inclination and 277° of azimuth (Figs. 15 and 16).

The safe mud window is defined as the area between the collapse pressure and the minimum horizontal stress. Figures 17, 18, 19, and 20 show the effects of the well inclination (Equivalent Mud Weight, EMW) on collapse pressure for the Kangan and Dalan Formations. Results show that the maximum horizontal stress requires a higher mud window. Parallel to the σ_H , Azimuths of 30° and 240° are likely to have higher mud weight. Similar to the issue of drilling inclination, a high mud weight will be required to overcome borehole collapse when drilling inclination increases borehole instability.

A significant challenge, when developing carbonate reservoirs, is the potential for abnormal pore pressures zones causing geological hazards (Khan et al. 2022). As abnormal (high) pore pressure enhances friction between formation and bit, it may contribute to wellbore instability issues, such as borehole collapse (Atashbari and Tingay 2012). Pore pressure variations in carbonates are caused by different types of porosity formed during diagenesis (fracturing and dissolution), depositional fabrics and deformation mechanisms (stress) (Khan et al. 2022). Pore pressure in carbonates is mostly caused by compaction disequilibrium regulated by the physical characteristics of the rock and pore fluids (Atashbari and Tingay 2012; Mohammed 2017). A variety of factors influence wellbore instability and the optimal mud weight in order to avoid sticking and borehole collapses, which cause borehole diameters to be smaller or larger and increase wellbore collapse in many formations such as shale and carbonate formations (Hoseinpour and Riahi 2022). This foundational information is crucial, particularly in the vicinity of faults and other geological complexities (Sanei et al. 2023). Identifying the magnitude and orientation of in situ stresses will aid drillers and reservoir engineers in determining the most appropriate safe trajectory for maximum productivity (Abdelghany et al. 2021; Bashmagh et al. 2022). Horizontal stresses calculations suffer from lack of leak-off test (LOT) or extended leak-off test (XLOT) data. In this regard, it was tried to optimize strain parameters (ϵ_x

Fig. 17 An analysis of collapse pressure (EMW) in terms of well inclination in K1 member, Kangan Formation

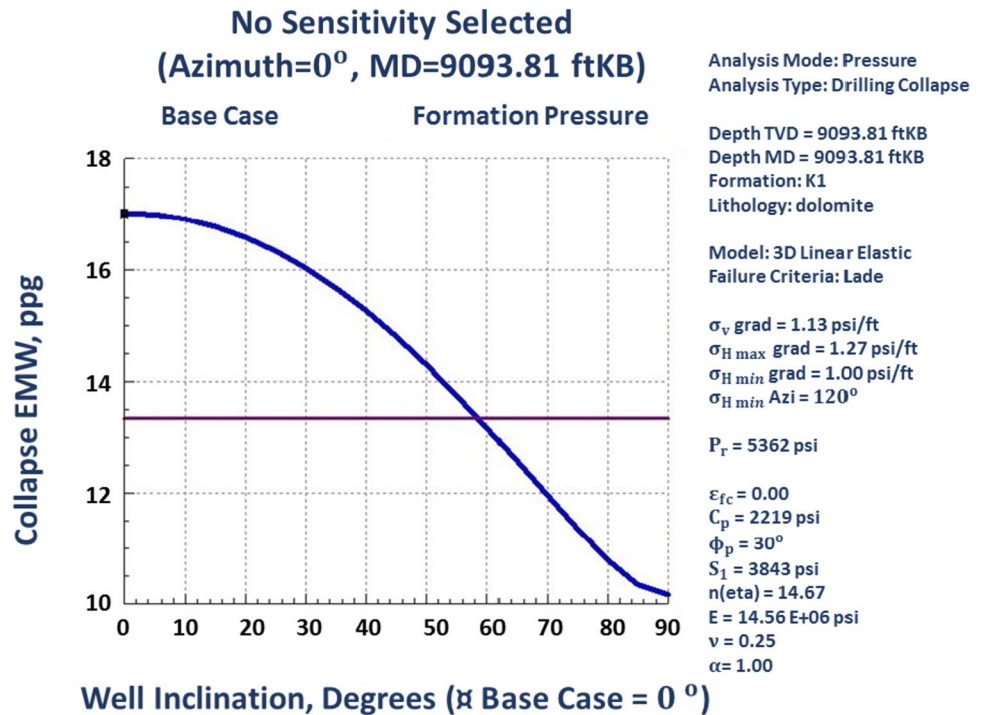
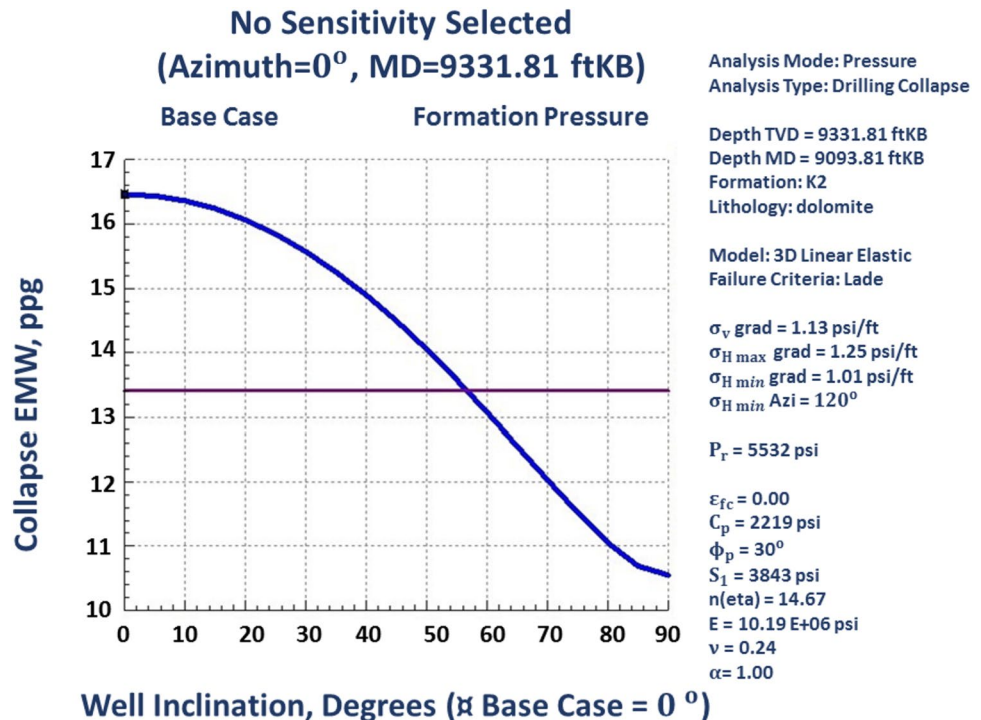


Fig. 18 Plot showing the effect of well inclination on collapse pressure in K2 member, Kangan Formation



and ϵ_y) until the mechanical earth models of the study area are well matched with field stress regime. Furthermore, the direction of horizontal strains can be inferred or verified using the full arm caliper data when borehole image logs are not available in all wells (Abdelghany et al. 2023). It was found that in the studied field, horizontal wells drilled

parallel to maximum horizontal stress (the most stable direction) where their stress anisotropy is the minimum (Peška and Zoback 1995). Khoshnevis-zadeh compared rock strength parameters with WOB instead of core data due to lack of availability (Khoshnevis-zadeh et al. 2019). Research on the investigated in situ stresses and wellbore

Fig. 19 Plot showing the effect of well inclination on collapse pressure in K3 member, Dalan Formation

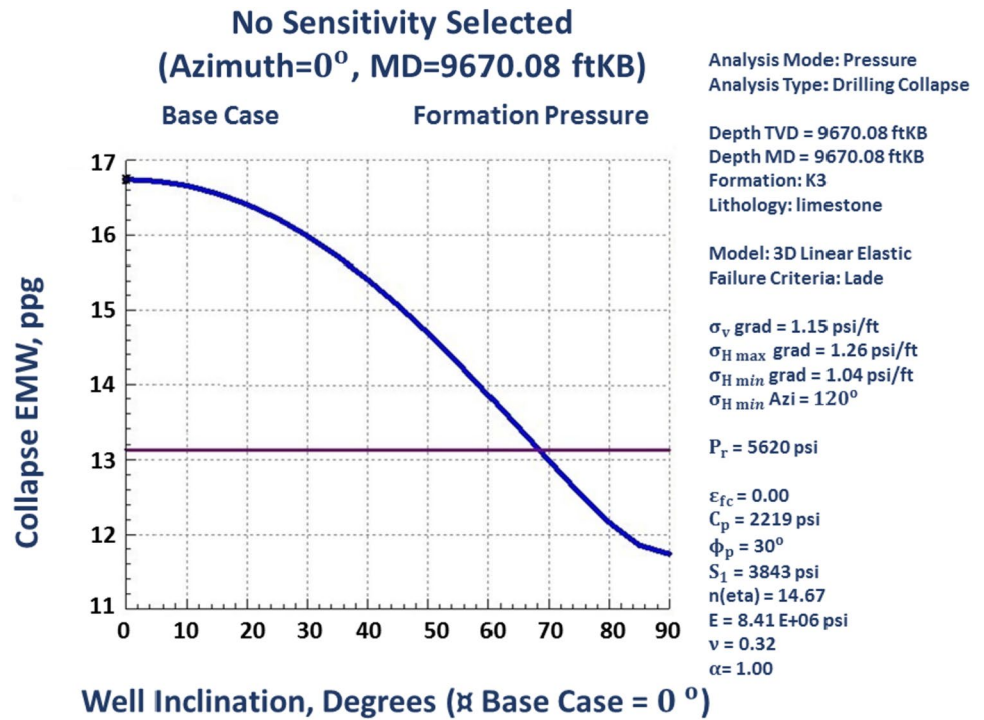
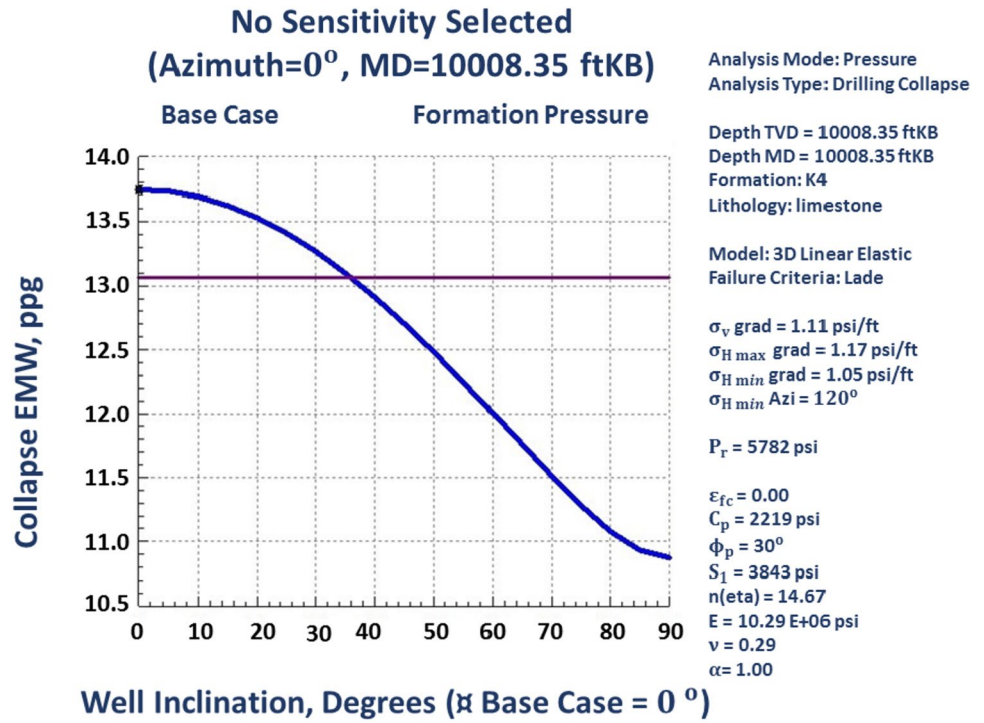


Fig. 20 Plot showing the effect of well inclination on collapse pressure in K4 member, Dalan Formation



stability analysis could provide valuable information for petroleum exploration and development and suggest possible areas for further exploration.

Conclusions

The current study showed a successful application of wellbore stability workflow on one of the gas wells of the Persian Gulf by using extensive data set of well logs, well test, and laboratory results. The following conclusions were reached.

- Stress calculations based on FMI logs showed that the stress regime is commonly strike-slip. Wellbore stability was analyzed using the Mohr–Coulomb failure criterion for the Kangan and Dalan Formations.
- According to the results, the mud weight applied in the Kangan and Dalan Formations was within a safe range. In addition, sensitivity analyses showed the optimal azimuth, deviation, and mud weight ranges. The optimal mud weights for the Kangan and Dalan Formations are 10–13 ppg and 11–14 ppg, respectively.
- Well azimuths in the NE–SW direction provide the best drilling stability in the studied carbonate formations.
- It was shown that the worst drilling direction that could lead to a high risk of wellbore instability is the azimuth of the minimum horizontal stress (σ_h). This is because drilling in this direction causes the pore pressure to exceed the tensile failure stress or fracture pressure, causing the wellbore to be damaged.
- It is recommended to develop a 3D/4D numerical model to improve the understanding of the relationships between field depletion and changes in stressed magnitude and orientation. Results of this research will help prevent borehole instability in the South Pars gas field and help drill similar wells in the future.
- The use of core samples and core data is very important for delivering reliable results, so we utilized three core samples and core data for the purpose of this study. In addition, using Eaton's method, pore pressure gradients were also calculated, that provided valuable information when calibrated with MDT results.

Author's contribution AS was involved in the methodology, software, data curation, visualization, writing—original draft, and writing—review and editing. AK contributed to the supervision, conceptualization, methodology, validation, and writing—review and editing. MN-B assisted in the supervision, conceptualization, validation, and writing—review and editing. MT contributed to the visualization and data curation.

Funding No funding was obtained for this study.

Declarations

Conflict of interest The authors declare that they have no known competing financial interests to personal relationships that could have appeared to influence the work reported in this study. This research did not receive any specific grants from public, commercial, or non-profit funding agencies.

Open Access This article is licensed under a Creative Commons Attribution 4.0 International License, which permits use, sharing, adaptation, distribution and reproduction in any medium or format, as long as you give appropriate credit to the original author(s) and the source, provide a link to the Creative Commons licence, and indicate if changes were made. The images or other third party material in this article are included in the article's Creative Commons licence, unless indicated otherwise in a credit line to the material. If material is not included in the article's Creative Commons licence and your intended use is not permitted by statutory regulation or exceeds the permitted use, you will need to obtain permission directly from the copyright holder. To view a copy of this licence, visit <http://creativecommons.org/licenses/by/4.0/>.

References

- Abdelghany WK, Radwan AE, Elkhawaga MA, Wood DA, Sen S, Kassem AA (2021) Geomechanical modeling using the depth-of-damage approach to achieve successful underbalanced drilling in the Gulf of Suez rift basin. *J Petrol Sci Eng* 202:108311. <https://doi.org/10.1016/j.petrol.2020.108311>
- Abdelghany WK, Hamed M, Radwan AE (2023) Implications of machine learning on geomechanical characterization and sand management: a case study from Hilal field, Gulf of Suez. *Egypt J Petrol Explorat Product Technol* 13(1):297–312. <https://doi.org/10.1007/s13202-022-01551-9>
- Abdideh M, Dastyaft F (2022) Stress field analysis and its effect on selection of optimal well trajectory in directional drilling (case study: southwest of Iran). *J Petrol Explorat Product Technol* 12(3):835–849. <https://doi.org/10.1007/s13202-021-01337-5>
- Abdideh M, Fathabadi MR (2013) Analysis of stress field and determination of safe mud window in borehole drilling (case study: SW Iran). *J Petrol Explorat Product Technol* 3(2):105–110. <https://doi.org/10.1007/s13202-013-0053-2>
- Almalikee HSA, Al-najim FMS (2018) Overburden stress and pore pressure prediction for the North Rumaila oilfield. *Iraq Modeling Earth Syst Environ* 4(3):1181–1188. <https://doi.org/10.1007/s40808-018-0475-4>
- Ashena R, Elmgerbi A, Rasouli V, Ghalambor A, Rabiei M, Bahrami A (2020) Severe wellbore instability in a complex lithology formation necessitating casing while drilling and continuous circulation system. *J Petrol Explorat Product Technol* 10(4):1511–1532. <https://doi.org/10.1007/s13202-020-00834-3>
- Ashena R, Roohi A, Ghalambor A (2022) Wellbore stability analysis in an offshore high-pressure high-temperature gas field revealed lost times due to lack of well trajectory optimization. *SPE Int Conf Exhibit Format Damage Control*. <https://doi.org/10.2118/208864-MS>
- Atashbari V, Tingay M (2012) Pore pressure prediction in a carbonate reservoir. SPE 150836. SPE Oil and Gas India conference and exhibition, Mumbai, India. <https://doi.org/10.2118/150836-MS>
- Awal M, Khan M, Mohiuddin M, Abdurraheem A, and Azeemuddin M (2001) A new approach to borehole trajectory optimisation for increased hole stability. In: SPE Middle East Oil Show. doi <https://doi.org/10.2118/68092-MS>

- Azadpour M, Shad Manaman N, Kadkhodaie-Ilkhchi A, Sedghipour MR (2015) Pore pressure prediction and modeling using well-logging data in one of the gas fields in south of Iran. *J Petrol Sci Eng* 128:15–23. <https://doi.org/10.1016/j.petrol.2015.02.022>
- Bagheri H, Tanha AA, Doulati Ardejani F, Heydari-Tajareh M, Larki E (2021) Geomechanical model and wellbore stability analysis utilizing acoustic impedance and reflection coefficient in a carbonate reservoir. *J Petrol Explorat Product Technol* 11(11):3935–3961. <https://doi.org/10.1007/s13202-021-01291-2>
- Bashmagh NM, Lin W, Murata S, Yousefi F, Radwan AE (2022) Magnitudes and orientations of present-day in-situ stresses in the Kurdistan region of Iraq: insights into combined strike-slip and reverse faulting stress regimes. *J Asian Earth Sci* 239:105398. <https://doi.org/10.1016/j.jseas.2022.105398>
- Bozorgi E, Javani D, Rastegarnia M (2016) Development of a mechanical earth model in an Iranian off-shore gas field. *J Mining Environ* 7:37–46. <https://doi.org/10.22044/jme.2016.457>
- Bradley, W. B. (1978). Bore hole failure near salt domes. In: SPE Annual Fall Technical Conference and Exhibition. <https://doi.org/10.2118/7503-MS>
- Croizet D, Renard F, Gratier JP (2013) Compaction and porosity reduction in carbonates: a review of observations, theory, and experiments. *Adv Geophys* 54:181–238. <https://doi.org/10.1016/b978-0-12-380940-7.00003-2>
- Darvishpour A, Seifabad MC, Wood DA, Ghorbani H (2019) Wellbore stability analysis to determine the safe mud weight window for sandstone layers. *Pet Explor Dev* 46(5):1031–1038. [https://doi.org/10.1016/s1876-3804\(19\)60260-0](https://doi.org/10.1016/s1876-3804(19)60260-0)
- Eaton BA (1976) Graphical method predicts geopressures worldwide. *World Oil*; (United States), 183(1). <https://www.osti.gov/biblio/7354696>
- Esrafilidizaji B, Rahimpour-bonab H (2019) Carbonate reservoir rocks at Giant oil and gas fields in Sw Iran and the adjacent offshore: a review of stratigraphic occurrence and poro-perm characteristics. *J Pet Geol* 42(4):343–370. <https://doi.org/10.1111/jpg.12741>
- Fjar E, Holt RM, Horsrud P, Raaen AM, Risnes R (2008) Chapter 3 geological aspects of petroleum related rock mechanics. *Developm Petrol Sci* 53: 103–133. doi [https://doi.org/10.1016/S0376-7361\(07\)53003-7](https://doi.org/10.1016/S0376-7361(07)53003-7)
- Gao Q, Cheng Y, Han S, Yan C, Jiang L (2019a) Numerical modeling of hydraulic fracture propagation behaviors influenced by pre-existing injection and production wells. *J Petrol Sci Eng* 172:976–987. <https://doi.org/10.1016/j.petrol.2018.09.005>
- Gao Q, Cheng Y, Han S, Yan C, Jiang L, Han Z, Zhang J (2019b) Exploration of non-planar hydraulic fracture propagation behaviors influenced by pre-existing fractured and unfractured wells. *Eng Fract Mech* 215:83–98. <https://doi.org/10.1016/j.engfractmech.2019.04.037>
- Gao Q, Han S, Cheng Y, Yan C, Sun Y, Han Z (2019c) Effects of non-uniform pore pressure field on hydraulic fracture propagation behaviors. *Eng Fract Mech* 221:106682. <https://doi.org/10.1016/j.engfracmech.2019.106682>
- Gholami R, Aadnoy B, Foon LY, Elochukwu H (2017) A methodology for wellbore stability analysis in anisotropic formations: a case study from the Canning Basin, Western Australia. *J Natural Gas Sci Eng* 37:341–360. <https://doi.org/10.1016/j.jngse.2016.11.055>
- Haimson B, Kovacich J (2003) Borehole instability in high-porosity Berea sandstone and factors affecting dimensions and shape of fracture-like breakouts. *Eng Geol* 69(3):219–231. [https://doi.org/10.1016/S0013-7952\(02\)00283-1](https://doi.org/10.1016/S0013-7952(02)00283-1)
- Han Y, Liu C, Phan D, Alruwaili K, Abousleiman Y (2019) Advanced wellbore stability analysis for drilling naturally fractured rocks. In: SPE middle east oil and gas show and conference. <https://doi.org/10.2118/195021-MS>
- Hashemi SS, Taheri A, Melkounian N (2014) Shear failure analysis of a shallow depth unsupported borehole drilled through poorly cemented granular rock. *Eng Geol* 183:39–52. <https://doi.org/10.1016/j.enggeo.2014.10.003>
- Heller R, Zoback M (2014) Adsorption of methane and carbon dioxide on gas shale and pure mineral. *J Unconvent Oil Gas Resour* 8:14–24. <https://doi.org/10.1016/j.juogr.2014.06.001>
- Hoseinipour M, Riahi MA (2022) Determination of the mud weight window, optimum drilling trajectory, and wellbore stability using geomechanical parameters in one of the Iranian hydrocarbon reservoirs. *J Petrol Explorat Product Technol* 12(1):63–82. <https://doi.org/10.1007/s13202-021-01399-5>
- Kadkhodaie A (2021) The impact of geomechanical units (GMUs) classification on reducing the uncertainty of wellbore stability analysis and safe mud window design. *J Natural Gas Sci Eng* 91:103964. <https://doi.org/10.1016/j.jngse.2021.103964>
- Kassem AA, Sen S, Radwan AE, Abdelghany WK, Abioui M (2021) Effect of depletion and fluid injection in the Mesozoic and Paleozoic sandstone reservoirs of the October oil field, central gulf of Suez basin: Implications on drilling, production and reservoir stability. *Nat Resour Res* 30(3):2587–2606. <https://doi.org/10.1007/s11053-021-09830-8>
- Khan MY, Awais M, Hussain F, Hussain M, Jan IU (2022) Pore pressure prediction in a carbonate reservoir: a case study from Potwar Plateau, Pakistan. *J Petrol Explorat Prod Technol* 12(11):3117–3135. <https://doi.org/10.1007/s13202-022-01511-3>
- Khatibi S, Aghajanzpour A, Ostadhasan M, Farzay O (2018) Evaluating single-parameter parabolic failure criterion in wellbore stability analysis. *J Natural Gas Sci Eng* 50:166–180. <https://doi.org/10.1016/j.jngse.2017.12.005>
- Khoshnevis-zadeh R, Soleimani B, Larki E (2019) Using drilling data to compare geomechanical parameters with porosity (a case study, South Pars gas field, south of Iran). *Arab J Geosci* 12(19):611. <https://doi.org/10.1007/s12517-019-4809-y>
- Khoshnevis-zadeh R, Hajian A, Larki E (2021) Pore pressure prediction and its relationship with rock strength parameters and weight on bit in carbonate reservoirs (a case study, South Pars gas field). *Arab J Sci Eng* 46(7):6939–6948. <https://doi.org/10.1007/s13369-020-05284-x>
- Kristiansen TG (2004) Drilling wellbore stability in the compacting and subsiding Valhall field. In: IADC/SPE drilling conference. doi <https://doi.org/10.2118/87221-MS>
- Martins AL, Santana ML, Gonçalves CJC, Gaspari E, Campos W, Perez JCLV (1999) Evaluating the transport of solids generated by shale instabilities in ERW drilling - part II: Case studies. In: SPE annual technical conference and exhibition. doi <https://doi.org/10.2118/56560-MS>
- Mohammed HQ (2017) Geomechanical analysis of the wellbore instability problems in Nahr Umr Formation southern Iraq. Missouri University of Science and Technology. https://scholarsmine.mst.edu/masters_theses/7695
- Mondal S, Chatterjee R (2019) Quantitative risk assessment for optimum mud weight window design: a case study. *J Petrol Sci Eng* 176:800–810. <https://doi.org/10.1016/j.petrol.2019.01.101>
- Moos D, Zoback MD (1990) Utilization of observations of well bore failure to constrain the orientation and magnitude of crustal stresses: application to continental, deep sea drilling project, and ocean drilling program boreholes. *J Geophys Res Solid Earth* 95(B6):9305–9325. <https://doi.org/10.1029/JB095iB06p09305>
- Peng S, Wang X, Xiao J, Wang L, Du M (2001) Seismic detection of rockmass damage and failure zone in tunnel. *J China Univ Min Tech* 30(1):23–26
- Peška P, Zoback MD (1995) Compressive and tensile failure of inclined well bores and determination of in situ stress and rock strength. *J Geophys Res Solid Earth* 100(B7):12791–12811. <https://doi.org/10.1029/95JB00319>

- Radwan AE (2021) Modeling pore pressure and fracture pressure using integrated well logging, drilling based interpretations and reservoir data in the Giant El Morgan oil Field, Gulf of Suez. *Egypt J African Earth Sci* 178:104165. <https://doi.org/10.1016/j.jafrearsci.2021.104165>
- Radwan A, Sen S (2021a) Stress path analysis for characterization of in situ stress state and effect of reservoir depletion on present-day stress magnitudes: reservoir geomechanical modeling in the Gulf of Suez Rift Basin. *Egypt Natl Resour Res* 30(1):463–478. <https://doi.org/10.1007/s11053-020-09731-2>
- Radwan AE, Sen S (2021b) Characterization of in-situ stresses and its implications for production and reservoir stability in the depleted El Morgan hydrocarbon field, Gulf of Suez rift basin. *Egypt J Struct Geol* 148:104355. <https://doi.org/10.1016/j.jsg.2021.104355>
- Radwan A, Abudeif A, Attia M, Mohammed M (2019) Pore and fracture pressure modeling using direct and indirect methods in Badri Field, Gulf of Suez. *Egypt African Earth Sci* 156:133–143. <https://doi.org/10.1016/j.jafrearsci.2019.04.015>
- Radwan A, Abudeif A, Attia M, Elkhawaga MA, Abdelghany WK, Kasem AA (2020) Geopressure evaluation using integrated basin modelling, well-logging and reservoir data analysis in the northern part of the Badri oil field, Gulf of Suez. *Egypt J African Earth Sci* 162:103743. <https://doi.org/10.1016/j.jafrearsci.2019.103743>
- Radwan AE, Abdelghany WK, Elkhawaga MA (2021) Present-day in-situ stresses in Southern Gulf of Suez, Egypt: insights for stress rotation in an extensional rift basin. *J Struct Geol* 147:104334. <https://doi.org/10.1016/j.jsg.2021.104334>
- Rahimi R (2014) The effect of using different rock failure criteria in wellbore stability analysis. Missouri University of Science and Technology. https://scholarsmine.mst.edu/masters_theses/7270
- Rahimpour-bonab H (2007) A procedure for appraisal of a hydrocarbon reservoir continuity and quantification of its heterogeneity. *J Petrol Sci Eng* 58(1–2):1–12. <https://doi.org/10.1016/j.petrol.2006.11.004>
- Sanei M, Ramezanzadeh A, Asgari A (2023) Building 1D and 3D static reservoir geomechanical properties models in the oil field. *J Petrol Explorat Prod Technol* 13(1):329–351. <https://doi.org/10.1007/s13202-022-01553-7>
- Talebi H, Alavi SA, Sherhati S, Ghassemi MR, Golalzadeh A (2018) In-situ stress regime in the Asmari reservoir of the Zelo and Lali oil fields, northwest of the Dezful embayment in Zagros fold-thrust belt Iran. *Geosciences* 106:53–68. <https://doi.org/10.22071/gsj.2018.58362>
- Tan C, Yaakub MA, Chen X, Willoughby D, Choi S, and Wu B (2004) Wellbore stability of extended reach wells in an oil field in Sarawak Basin, South China Sea. In: SPE Asia Pacific oil and gas conference and exhibition. doi <https://doi.org/10.2118/88609-MS>
- Zang A, Stephansson O (2009) Stress field of the Earth's crust. Springer Science and Business Media. <https://doi.org/10.1007/978-1-4020-8444-7>
- Zoback MD (2010) Reservoir geomechanics. Cambridge University Press. <https://doi.org/10.1017/CBO9780511586477>

Publisher's Note Springer Nature remains neutral with regard to jurisdictional claims in published maps and institutional affiliations.